Perfluorooctyl Bromide Has Limited Membrane Solubility and Is Located at the Bilayer Center. Locating Small Molecules in Lipid Bilayers through Paramagnetic Enhancements of NMR Relaxation

Jeffrey F. Ellena,[†] Viktor V. Obraztsov,[‡] Valerie L. Cumbea,[†] Catherine M. Woods,[‡] and David S. Cafiso*[,†]

Department of Chemistry and Biophysics Program, University of Virginia, Charlottesville, Virginia, and Department of Biological Research, Alliance Pharmaceutical Corporation, San Diego, California

Received July 1, 2002

There is considerable interest in the use of perfluorocarbons as oxygen carriers in clinical settings; however, little is known regarding the molecular interactions made by these apolar compounds with biological membranes or their effect on membrane structure. NMR spectroscopy was used to investigate the interaction of perfluorooctyl bromide (PFOB) with 1-palmitoyl-2-oleoyl-*sn*-glycero-3-phosphocholine (POPC) bilayers. ^{19}F NMR spectra demonstrate that PFOB partitions into POPC bilayers but that it saturates at a remarkably low membrane concentration of approximately 2 mol %. ^{19}F chemical shifts indicate that this membrane-bound PFOB experiences a local environment similar in polarity to that of hexane, suggesting that the compound resides within the hydrocarbon core of the lipid bilayer. This hydrocarbon location was refined by measuring paramagnetic enhancements of ^{19}F nuclear relaxation for membrane-bound PFOB produced by Gd^{3+} and O_2. The data clearly localize PFOB to the center of the membrane hydrocarbon and show how paramagnetic enhancements of nuclear relaxation produced by O_2 may be used to localize small molecules within bilayers. ^2H and ^{31}P NMR experiments demonstrate that PFOB produces no significant changes in either acyl chain or headgroup structure even at saturating membrane concentrations.

Introduction

Perfluorocarbons (PFCs) have been evaluated as oxygen carriers in a variety of clinical settings because they readily solubilize gases.[1−4] Perfluorooctyl bromide (PFOB) is a dense, biochemically inert liquid with a high spreading coefficient and is highly hydrophobic and only weakly lipid soluble.[1,4−6] Following in vivo administration, PFOB is not metabolized and is eliminated as vapor from the body by exhalation via the lung. In addition to being evaluated as an intravenous emulsion for temporary oxygen transport during surgery,[7,8] it is also being evaluated in conjunction with a technique known as partial liquid ventilation (PLV) for patients with acute respiratory distress syndrome (ARDS).[6,9,10] PLV with PFOB has been shown to improve gas exchange to a greater extent than simple gas ventilation in a variety of preclinical animal models of acute lung injury.[2,3,9,11] In parallel, a reduction in lung inflammation as manifested by reductions in neutrophil influx, alveolar hemorrhage, and vascular leakage is observed. While PLV with PFOB appears to attenuate lung injury that can occur during conventional mechanical ventilation,[6,12,13] PFOB also appears to attenuate a variety of proinflammatory responses in vitro.[14−16] Recent studies have indicated that some of these effects may be in part related to the lipid solubility of the PFC and that the effects on erythrocyte osmotic responses and platelet aggregation responses correlate with the lipid solubility of the PFC.[17]

Despite their clinical importance, there is virtually no information on the interactions made by perfluorcarbons such as PFOB with lipid bilayers. These molecules are hydrophobic, and they have some lipid solubility. As a result, they may alter the dynamics or packing of lipids within membranes. Previous studies have been carried out on smaller but related halogenated and perfluorinated compounds that violate the Meyer−Overton rule. These compounds are sometimes referred to as nonimmobilizers, and they violate the Meyer−Overton rule because they exhibit strong membrane partitioning but lack anesthetic potency.[18] These nonimmobilizers localize differently than do anesthetics in membranes; anesthetic compounds tend to localize at the membrane interface whereas the nonimmobilizers reside within the membrane hydrocarbon.[19,20] Remarkably, nonimmobilizers have no measurable effect on membrane hydrocarbon packing or acyl chain dynamics.

In the present study, we report measurements directed at determining the partitioning and membrane distribution of PFOB as well as its effect on lipid packing. These measurements are performed in fluid-phase model membrane systems formed from palmitoyloleoylphosphatidylcholine (POPC) and make use of bilayer oxygen gradients to produce paramagnetic enhancements in nuclear relaxation. PFOB is found to localize within the central hydrocarbon core, but it has surprisingly limited membrane solubility. At saturating concentrations, this compound has no measurable effect on lipid chain dynamics or lipid headgroup conformation.

* To whom correspondence should be addressed. Address: Department of Chemistry, P.O. Box 400319, University of Virginia Charlottesville, VA 22904-4319. Phone: 434-924-3067. Fax: 434-924-3710. E-mail: cafiso@virginia.edu.
[†] University of Virginia.
[‡] Alliance Pharmaceutical Corporation.

10.1021/jm020278x CCC: $22.00
Published on Web 11/07/2002

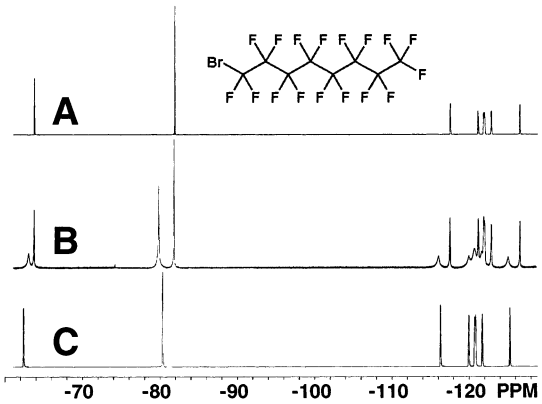

Figure 1. Structure of PFOB and ^{19}F NMR spectra: (A) neat PFOB; (B) PFOB in micelles and in POPC bilayer vesicles; (C) PFOB in hexanes. All spectra were recorded at 37 °C.

Table 1. Chemical Shifts for Neat PFOB, Micellar PFOB, PFOB Bound to POPC Bilayers, and PFOB in Hexane

position	neat PFOB[a]	micellar PFOB[a]	bilayers and bound PFOB[a]	5% PFOB in hexane[a]
1	−63.83	−63.85	−63.01	−62.41
2	−117.59	−117.6-	−116.08	−116.28
3	−121.18	−121.19	−119.95	−119.94
4	−121.90	−121.93	−120.70	−120.70
5	−122.91	−122.92	−121.70	−121.68
6	−129.91	−129.92	−121.60	−121.68
7	−126.61	−126.62	−125.05	−125.26
8	−81.93	−81.94	−79.93	−80.34

[a] In ppm relative to external $CFCl_3$. Temperature is 37 °C.

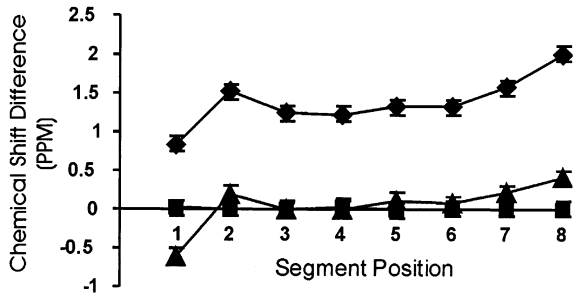

Figure 2. ^{19}F chemical shift differences between PFOB bound to POPC bilayers and PFOB micelles in aqueous solution (◆), neat PFOB and PFOB micelles in aqueous solution (■), and PFOB bound to POPC bilayers and PFOB in hexanes (▲).

Results

Chemical Shifts Reveal Partitioning and Saturable Binding of PFOB to Bilayers. Figure 1A shows the ^{19}F spectrum and structure of neat PFOB. In the ^{19}F NMR spectrum, eight resonance peaks are observable, one for each carbon position. The peak assignments and chemical shifts are listed in Table 1. These resonance assignments were made previously[21] but were confirmed here using ^{19}F double-quantum-filtered correlation spectroscopy (COSY).

Shown in Figure 1B is a spectrum of POPC bilayers containing 3 mol % PFOB. This spectrum has two sets of resonances, one with chemical shifts nearly identical to those observed for neat PFOB (Figure 1A and Table 1) and a second set that is broader with chemical shifts similar to those observed for PFOB in hexanes (Figure 1C and Table 1). Figure 2 contains a summary of three sets of chemical shift differences: PFOB in the presence of bilayers versus PFOB micelles in aqueous solution, neat PFOB versus PFOB micelles in aqueous solution, and PFOB in the presence of bilayers versus 5% PFOB in hexanes. The chemical shift similarity of the broad PFOB resonances, particularly those due to positions 3−6, to the analogous resonances of PFOB in hexanes suggests that the broad resonances are due to PFOB that is in a hydrocarbon environment, presumably within the lipid bilayer hydrocarbon.

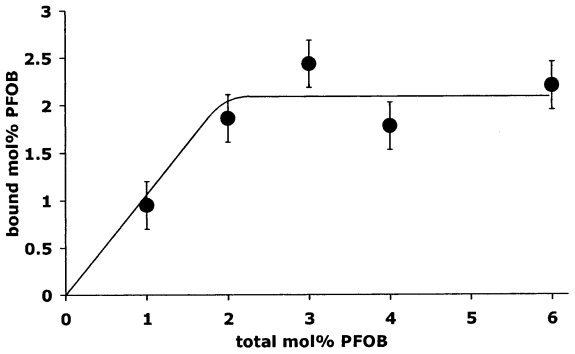

Figure 3. PFOB binding to POPC large unilamellar vesicles. Bound versus total mol % PFOB is plotted.

To determine which ^{19}F resonances were arising from PFOB that was membrane-associated, ^{19}F NMR spectra were recorded for bilayers and supernatant following centrifugation of POPC bilayers in D_2O containing 3 mol % PFOB. The spectrum of the centrifuged bilayers was dominated by the broad resonances shown in Figure 1B, while the ^{19}F NMR spectrum of the clear supernatant was dominated by narrow peaks having chemical shifts similar to those observed for neat PFOB. The distribution of resonance intensity in the bilayer and supernatant confirms that the broad resonances are due to PFOB that is bound to the POPC bilayers, while the set of narrow resonances is associated with PFOB micelles in solution. PFOB must be present in solution in a micellar form because the chemical shifts in solution are virtually identical to those seen for neat PFOB (see Figure 2) and because the aqueous solubility of PFOB is below the limit of detection for the present ^{19}F NMR experiments.[1] ^{19}F chemical shifts are highly dependent on environment, and the similarity of the chemical shifts for PFOB bound to bilayers to those seen for PFOB in the presence of hexane suggests that PFOB is located in the hydrocarbon region of the POPC bilayers. The ^{19}F resonances due to bilayer-bound PFOB are broader than the neat PFOB or PFOB micelle resonances because the reorientation of bound PFOB is slower than neat or micellar PFOB reorientation.

By use of ^{19}F NMR, the incorporation of PFOB into lipid bilayers was followed as a function of the total concentration of PFOB. Under the conditions of this experiment, the lipid is present at high concentrations and PFOB partitions completely into bilayers at low levels of PFOB. Figure 3 shows the mole fraction of PFOB incorporated into POPC as a function of concentration. At low levels, PFOB is completely associated with POPC bilayers; however, saturation is reached at 2 mol % and further addition of PFOB results in the formation of PFOB micelles. A very similar binding curve was generated independently using gas chromatography (data not shown). The ^{19}F line widths due to PFOB bound to bilayers are constant over the PFOB

concentration range studied, suggesting that the aggregation state of bound PFOB is independent of PFOB concentration. It should be noted that because the aqueous solubility of PFOB is very low,[1] the monomer concentration of PFOB in solution is much lower than the concentration of PFOB in bilayers.

Paramagnetic Enhancements of NMR Relaxation Produced by Gd^{3+} and O_2 Localize PFOB to the Bilayer Center. To obtain additional information on the membrane location of PFOB, we examined the effect of gadolinium and molecular oxygen on PFOB spin−lattice relaxation. Gd^{3+} has been shown to bind to the phosphate moiety of bilayer phospholipids, and because it is paramagnetic, it enhances nuclear spin relaxation in a distance-dependent manner.[22] Molecular oxygen is also paramagnetic but is concentrated in the hydrocarbon core of the bilayer.[23,24] We measured relaxation enhancements due to Gd^{3+} and O_2 for the ^{13}C resonances of POPC and the ^{19}F resonances of perfluorooctanoic acid (PFOA). These data yielded a relationship between relaxation enhancement and intrabilayer segmental location. We then measured analogous relaxation enhancements for the ^{19}F resonances of PFOB and were able to interpret them in terms of intrabilayer location.

The ^{13}C spin−lattice relaxation rate enhancement (T_{1para}^{-1}) promoted by different concentrations of Gd^{3+} in POPC is shown in Figure 4A, and as expected, the largest observable enhancement occurs at the headgroup methylene adjacent to the phosphate (choline α-CH_2). When 0.5 or 1.5 mM Gd^{3+} is present, enhancements at the choline α-CH_2 are 9- and 27-fold greater than the unenhanced rate. Relaxation enhancements for the glycerol carbons could not be measured because of the large line broadening and consequent reduction in signal-to-noise caused by Gd^{3+}. Substantial enhancements were seen for other positions located near the POPC phosphate group, and the size of the enhancements decreased as the distance between the POPC phosphate and the enhanced nucleus increased. Enhancements observed for the fatty acyl chain methylenes and methyl groups were much smaller than those observed in the headgroup. The positional dependence of these enhancements is consistent with Gd^{3+} binding to the POPC phosphate group.

The effect of Gd^{3+} on ^{19}F intrabilayer PFOB spin−lattice relaxation is shown in Figure 4B. Gd^{3+} had no effect on micellar PFOB relaxation (not shown). The presence of 0.5 mM Gd^{3+} caused a small (7−20%) T_1^{-1} increase for all positions of PFOB bound to POPC. When larger amounts of Gd^{3+} were added to bilayers containing PFOB, larger T_{1para}^{-1} are observed (Figure 4B). The portion of the relaxation rate caused by Gd^{3+} is substantial above 0.5 mM Gd^{3+} with Gd^{3+} enhancement accounting for approximately 19−36% and 41−52% of the total rate at 1.5 and 5 mM Gd^{3+}, respectively. The increase in PFOB relaxation due to the presence of Gd^{3+} at all Gd^{3+} concentrations studied (Figure 4B) was much smaller than that observed in the POPC headgroup (Figure 4A). This observation indicates that the bound PFOB is not located in the headgroup or glycerol backbone region of the POPC bilayers and therefore must be in the hydrocarbon region.

Intermolecular nuclear spin−lattice relaxation enhancement due to an unpaired electron spin is proportional to γ_I^2/b^3 (see Appendix), where γ_I is the nuclear magnetogyric ratio and b is the distance of closest approach of the electron and nuclear spins. Thus, one can use the ratio $(\gamma_C^2\, b_F^3)/(\gamma_F^2 b_C^3)$ to convert ^{19}F spin−lattice relaxation rates due to intermolecular dipolar interactions to ^{13}C rates. We used the ^{19}F PFOB spin−lattice relaxation rate enhancements obtained in the presence of 1.5 mM Gd^{3+} to estimate analogous ^{13}C rates. These ^{13}C rate enhancements can then be compared with those obtained for POPC acyl chain resonances to yield information on the location of PFOB that is bound to POPC bilayers. Figure 5A is a plot of POPC acyl chain and PFOB ^{13}C spin−lattice relaxation rate enhancements due to 1.5 mM Gd^{3+}. The POPC headgroup and glycerol ^{13}C rate enhancements are considerably higher than those observed for the acyl chain region (Figures 4A and 5A). POPC acyl chain ^{13}C rate enhancements for those segments located closer to the center of the bilayer than the second methylene from the carboxyl group are similar to each other and relatively small. The PFOB ^{13}C rate enhancements are similar to each other and approximately 10 times lower than the smallest POPC acyl chain ^{13}C rate enhancements. The PFOB and POPC acyl chain ^{13}C rate enhancements are consistent with a bilayer hydrocarbon location for PFOB. Detailed quantitative comparison of the PFOB and POPC ^{13}C

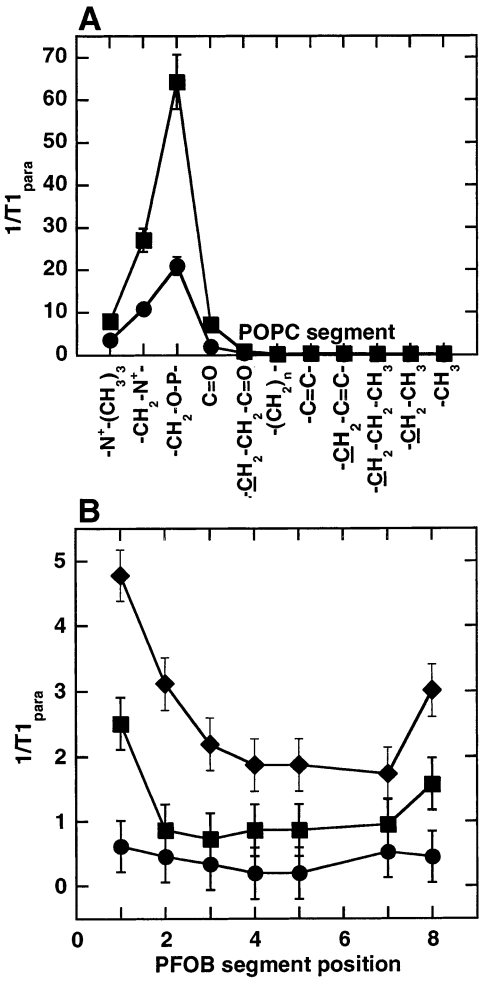

Figure 4. (A) POPC ^{13}C spin−lattice relaxation enhancements induced by 0.5 (●) or 1.5 mM (■) Gd^{3+}. POPC segment positions are shown on the x axis. (B) ^{19}F spin−lattice relaxation enhancements for PFOB bound to POPC. Enhancements were induced by 0.5 (●), 1.5 (■), or 5 mM (◆) Gd^{3+}.

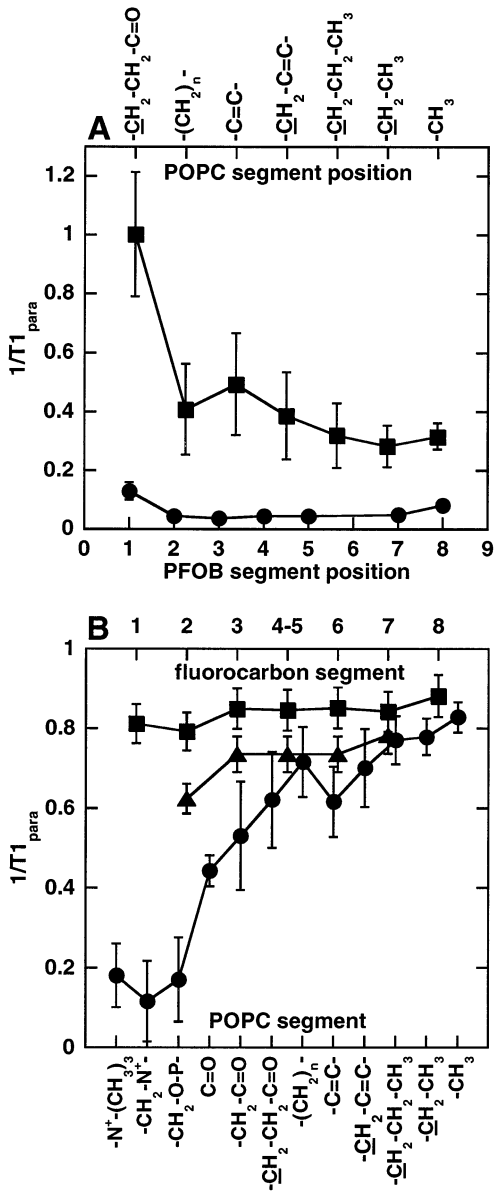

Figure 5. (A) ^{13}C spin−lattice relaxation enhancements for PFOB (●) and POPC (■) due to 1.5 mM Gd^{3+} at 37 °C. (B) ^{13}C spin−lattice relaxation enhancements for PFOB (■), PFOA (▲), and POPC (●) due to 17 atm of O_2 at 25 °C.

rate enhancements due to Gd^{3+} is not possible for reasons that will be discussed below.

The paramagnetic enhancement of PFOB, PFOA, and POPC nuclear spin−lattice relaxation by molecular oxygen was measured and is shown in Figure 5B. Here, the ^{19}F relaxation rates have been converted to ^{13}C rates as described above. The dependence of the oxygen-induced relaxation rate enhancements on POPC segment position primarily reflects the bilayer O_2 gradient. Relaxation enhancement is smallest for the headgroup nuclei and increases as one proceeds to the methyl ends of the acyl chains. Nuclear relaxation rate enhancements are proportional to oxygen−nuclear proximities and therefore comparison of PFOB and PFOA rates with those of POPC will indicate the intrabilayer locations of PFOB and PFOA relative to POPC. The rate enhancements observed for PFOA are similar to those observed for the analogous positions of the POPC acyl chains. PFOA positions 3−6 overlap in the ^{19}F spectrum,

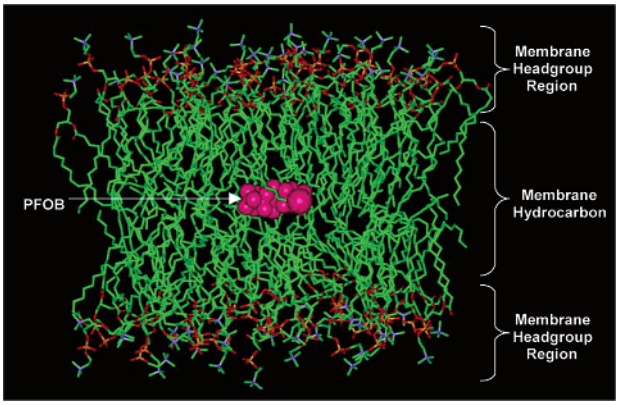

Figure 6. Location of PFOB in POPC bilayers. The POPC bilayer coordinates were obtained from Scott Feller (http://persweb.wabash.edu/facstaff/fellers/coordinates/popc.pdb). The PFOB was energy-minimized and placed in a bilayer location that is consistent with chemical shift and relaxation data.

and only a single relaxation time can be measured for these positions. Two partially overlapping peaks were observed for position 8 due to the asymmetry of the inner and outer leaflets of the bilayer. The measured relaxation at this position was not a single exponential, and consequently, this position was not included in our analysis. The PFOA is almost fully unprotonated under our experimental conditions (pH 8), and consequently, one would expect that PFOA would occupy a bilayer location that is similar to that of the POPC acyl chains. The relaxation data support the expected PFOA location. The PFOB nuclear spin−lattice relaxation rate enhancements due to oxygen (Figure 5B) are somewhat greater than those observed for PFOA and are the same as those observed near and at the end of the POPC acyl chain. Thus, the average intrabilayer location of PFOB is near the bilayer center as shown schematically in Figure 6.

PFOB Has No Effect on the Headgroup or Acyl Chain Configuration of POPC Bilayers. Multilamellar dispersions containing PFOB and deuterated phosphatidylcholine were prepared in order to assess the effect of PFOB on bilayer phosphatidylcholine conformation. Lipids deuterated exclusively in the headgroup (choline perdeuterated DMPC-d_{13} or choline α-POPC-d_2) or *sn*-1 acyl chain position (*sn*-1 palmitoyloleoylphosphatidylcholine-d_{31}) were used. The phosphatidylcholine dispersions contained 0, 2.5, 5, or 20 mol % PFOB, and ^2H and ^{31}P spectra were collected at 25 and 37 °C. The ^2H quadrupolar splittings and ^{31}P residual chemical shift anisotropies were measured as described in Experimental Section. The ^2H and ^{31}P NMR data are in the Supporting Information. Most ^2H quadrupolar splittings are unchanged (within experimental error) in the presence of high levels of PFOB. In a few cases, small changes that are on the order of 1% can be observed. A large body of work has shown that these quadrupolar splittings reflect acyl chain dynamic conformation and are related to acyl chain length, area, and configuration; they are highly sensitive indicators of bilayer structure.[25−27] The data indicate that PFOB, when present at levels of up to 20 mol %, has no significant effect on the structure of POPC bilayers at 25 and 37 °C.

Discussion

One of the goals of the current study was to determine whether PFOB has an effect on lipid bilayer structure or organization, and we examined both the acyl chain and headgroup regions of the bilayer. The data show that high levels of PFOB have virtually no effect on lipid bilayer structure and the lack of an effect of PFOB on bilayer structure is likely due to its low level of incorporation. Data obtained here from ^{19}F NMR indicate that PFOB saturates in POPC bilayers at approximately 2 mol % and that subsequent addition of this compound results in the formation of PFOB micelles within the aqueous phase. The formation of these two pools of PFOB can easily be seen in Figure 1B, and resolution of these pools in the spectrum indicates that the exchange of PFOB is slow on the NMR time scale (10^{-6} s). This remarkable result is not entirely unexpected. PFOB is somewhat lipophobic, having a limited solubility in olive oil of 37 mM (or approximately 10 mol %).[1] The formation of micelles in solution at higher concentrations is consistent with the observation that PFOB is very hydrophobic and its monomeric form has very low water solubility ($\sim 10^{-9}$ M).

When bound to lipid bilayers, the ^{19}F shifts of the PFOB fluoromethylene groups (particularly positions 3−6) in POPC bilayers are very similar to those of PFOB in hexane; therefore, it is likely that PFOB is located in the hydrocarbon region of the bilayer. Enhancements of nuclear spin relaxation by Gd^{3+} and molecular oxygen were used to further assess the bilayer location of PFOB. Bilayer POPC ^{13}C relaxation rate enhancements due to Gd^{3+} (Figure 4A) are consistent with previous work indicating that the Gd^{3+} binds to the POPC phosphate group.[22] While interactions between Gd^{3+} and POPC headgroup nuclei are likely to be primarily intramolecular, interactions between Gd^{3+} and POPC acyl chain nuclei are likely to be primarily intermolecular, as is the case for dipolar interactions between headgroup and acyl chain ^1H in bilayers.[28,29] The measured ^{19}F PFOB relaxation enhancements can be used to calculate analogous ^{13}C enhancements as shown in the Appendix, facilitating comparison of PFOB and POPC enhancements and identification of the binding location of PFOB in bilayers. Comparison of Figures 4A and 5A shows that the PFOB enhancements due to Gd^{3+} are several orders of magnitude smaller than those observed for the POPC headgroup. Therefore, PFOB is not located in the headgroup or glycerol region of POPC bilayers and therefore must be located in the bilayer acyl chain region. Inspection of Figure 5A shows that the smallest POPC enhancements are about an order of magnitude greater than the PFOB enhancements. This observation suggests that PFOB is located near the center of the bilayer. Unfortunately comparison of Gd^{3+}-induced ^{13}C PFOB and POPC relaxation enhancements cannot provide high-resolution structural information because the difference in the translational diffusion rate of the Gd^{3+}−POPC and Gd^{3+}−PFOB electron−nuclear vectors is unknown and because the Gd^{3+}−POPC acyl chain and the Gd^{3+}−PFOB distances of closest approach are not known.

More precise information about the location of PFOB in the bilayer hydrocarbon region was obtained from nuclear spin−lattice relaxation experiments in the presence and absence of O_2. Molecular oxygen is paramagnetic and more soluble in hydrocarbon solvents than in aqueous solutions. Previous studies have shown that an O_2 concentration gradient exists in lipid bilayers where the O_2 concentration at the bilayer center is higher than at the bilayer interface.[23,24] Oxygen concentration gradients have been used to determine the membrane localization of proteins using site-directed spin labeling,[30] and intrabilayer locations of ^{19}F-labeled molecules can be determined by examining the effect of O_2 on ^{19}F spin−lattice relaxation rates.[31,32]

We have examined the effect of pressurized (17 atm) O_2 on PFOB and PFOA ^{19}F and POPC ^{13}C spin−lattice relaxation rates. The ^{19}F PFOB and PFOA relaxation enhancements can be converted to equivalent ^{13}C enhancements (see Appendix) in order to facilitate a comparison with the ^{13}C POPC enhancements. This conversion of ^{19}F to ^{13}C rates was shown to be valid by comparing ^{19}F and ^{13}C data for neat PFOB. The ^{13}C rate enhancements for PFOB, PFOA, and POPC will all be directly proportional to O_2−^{13}C proximities (eq 4, Appendix), and the POPC enhancements can be used for a bilayer depth calibration because the locations of the POPC ^{13}C nuclei in bilayers are well-characterized. Thus, by comparison of PFOB and PFOA ^{13}C O_2 enhancements to those for POPC, the positions of nuclei for PFOB or PFOA in bilayers can be obtained.

The ^{13}C PFOB, PFOA, and POPC relaxation enhancements due to O_2 are shown in Figure 5B. Because the POPC enhancements are proportional to the O_2 concentration, the POPC data in Figure 5B are a profile of the O_2 concentration across the bilayer. The transbilayer O_2 profile in Figure 5B qualitatively agrees with the transbilayer polarity profile obtained by White and coworkers for DOPC based on X-ray and neutron diffraction data[33] and the transmembrane oxygen concentration profile for rod outer segment disks.[23] The O_2-induced ^{13}C relaxation enhancement for PFOA is similar to that observed for the POPC acyl chains, and the data in Figure 5B allow one to structurally distinguish the molecular segments in the bilayer hydrocarbon region that are closer to the aqueous-hydrocarbon interface from those that are closer to the center of the bilayer. Taken together, the PFOA enhancements suggest that the PFOA occupies a bilayer position that is similar to that occupied by the POPC acyl chains. This PFOA location is similar to those found in other studies of other fatty acids.[34] Thus, the determined PFOA location supports the validity of our localization method.

The O_2-induced ^{13}C PFOB relaxation enhancements for all positions are similar to each other, larger than the PFOA enhancements, and similar to the enhancements observed in the last three segments of the POPC acyl chains (Figure 5B). We have also examined the effect of O_2 on ^{13}C POPC and ^{19}F PFOB chemical shifts[31,32,35] (data not shown), and the results are in agreement with the analogous relaxation data. The ^{13}C POPC shifts due to 17 atm of O_2 gradually increase as one proceeds from the carbonyl to the methyl end of the fatty acyl chains. The ^{19}F PFOB shifts for all positions are similar (standard deviation is ±5%; maximum difference is 13%), and when normalized to ^{13}C, they are similar to the three carbons at the methyl end of the acyl chains. The effect of O_2 on both relaxation and

chemical shifts indicates that the average location of PFOB is the center of the bilayer as shown in Figure 6. Owing to the dynamic nature of the bilayer hydrocarbon region, it is likely that there is some distribution of PFOB intrabilayer locations; however, our data do not allow us to assess that distribution. The PFOB intrabilayer location is consistent with the very low solubility of PFOB in water ($\sim 10^{-9}$ M) and molecular dynamics simulations that indicate a lower interfacial attraction for CF_2 and CF_3 groups relative to CH_2 and CH_3 groups, respectively.[36]

Prosser and co-workers have pioneered the use of transbilayer oxygen concentration gradients and ^{19}F NMR to obtain high-resolution structural information on molecules residing in membranes.[31,32,35] They have related O_2-induced relaxation enhancement to membrane depth by measuring the relaxation enhancement of different cholesterols having ^{19}F atoms at known membrane depths and fitting the results to a Gaussian function.[32] Our work differed from that of Prosser in that we related relaxation enhancement to membrane depth by measuring bilayer phospholipid ^{13}C relaxation and assumed no functional form for the relationship between relaxation enhancement and bilayer depth. Advantages of our approach include the facts that no specific labeling of molecules and no functional form for the transbilayer oxygen gradient are required for establishing the relationship between relaxation enhancement and membrane depth. Our approach has the disadvantages that one must use relaxation theory to convert ^{19}F relaxation rates to ^{13}C rates, and owing to the smaller magnetgyric ratio for ^{13}C, the O_2-induced ^{13}C relaxation enhancements are smaller than analogous ^{19}F enhancements.

The behavior of PFOB is similar to that observed for some fully halogenated molecules such as 1,2-dichlorohexafluorocyclobutane, which violate the Meyer−Overton rule.[18,19] The Meyer−Overton rule predicts that a molecule's anesthetic potency will be proportional to its solubility in hydrocarbons such as olive oil; however, molecules such as 1,2-dichlorohexafluorocyclobutane partition strongly into hydrocarbon phases but have little or no anesthetic activity (they are referred to as nonimmobilizers). Like PFOB, these nonimmobilizers locate within the hydrocarbon core of the bilayer and have little effect upon acyl chain conformation. The membrane location obtained here for PFOB is consistent with the fact that PFOB does not obey the Meyer−Overton rule and is a nonimmobilizer.

In summary, ^{19}F NMR provides clear evidence that PFOB has limited solubility in lipid bilayers and that it saturates the bilayer at a concentration of approximately 2 mol %. A careful examination of bilayers using ^{2}H and ^{31}P NMR indicates that PFOB has no measurable effect on bilayer conformation even at levels that vastly exceed membrane saturation. Paramagnetic enhancements produced by Gd^{3+} and O_2 demonstrate that PFOB is localized in the center of the hydrocarbon core when membrane-bound, a result that is agreement with the ^{19}F chemical shifts of membrane-associated PFOB. Despite the highly hydrophobic nature of perfluorocarbons, these results suggest that compounds such as PFOB are remarkably inert toward lipid bilayers.

Experimental Section

Abbreviations. PFOA, perfluorooctanoic acid; PFOB, perfluorooctyl bromide; POPC, 1-palmitoyl-2-oleoyl-*sn*-glycero-3-phosphocholine; PFC, perfluorocarbon; PLV, partial liquid ventilation; ARDS, acute respiratory distress syndrome; SUV, small unilamellar vesicle; T_{1para}^{-1}, spin−lattice relaxation rate due to paramagnetic species; T_{1intra}^{-1}, spin−lattice relaxation rate due to intramolecular interactions; T_{1inter}^{-1}, spin−lattice relaxation rate due to intermolecular interactions.

Sample Preparation and ^{13}C and ^{19}F NMR. All lipids were obtained from Avanti Polar Lipids (Alabaster, AL). Medical grade PFOB was supplied by Alliance Pharmaceutical Corp. (San Diego, CA). Hexanes (reagent grade), PFOA, and $GdCl_3$ were from Aldrich (Milwaukee, WI). Dry POPC was dispersed in 10 mM K_2HPO_4, pH 7 (5% H_2O, 95% D_2O). Samples containing a range (1−20 mol %) of PFOB concentrations were prepared by adding an appropriate amount of PFOB to each sample. The final POPC concentration was 50 mM. Samples were mechanically mixed and then frozen and thawed seven times. Finally samples were extruded through a 0.1 μm pore filter (Poretics, Osmonics Inc.) 20 times. The final sample volume was 4 mL, and the samples were transferred to 10 mm NMR tubes (513-7PP, Wilmad Glass, Buena, NJ). All measurements of PFOB binding to POPC were made at 37 °C. The effect of gadolinium (Gd^{3+}) on phospholipid ^{13}C and PFOB ^{19}F spin−lattice relaxation was examined by preparing samples in the same way as described above with the following exceptions. The POPC concentration was 100 mM, and no buffer was used. Appropriate amounts of 50 mM $GdCl_3$ were added to the hydrated POPC before freeze−thawing. The effect of pressurized molecular oxygen (O_2) on ^{19}F and ^{13}C spin−lattice relaxation in neat PFOB and POPC bilayers containing PFOB or PFOA was examined.[31,32] An aliquot of PFOA in methanol was dried in a conical centrifuge tube, and 2 mL of 100 mM POPC hydrated with 10 mM K_2HPO_4, pH 8 (5% H_2O, 95% D_2O), was added. The mixture was vortexed and then freeze−thawed seven times. Subsequently the bilayers were briefly (3 × 30 s) sonicated with a probe sonicator (Heat Systems, Farmingdale, NY). Unsonicated lipid and sonicator tip particles were separated from small unilamellar vesicles (SUV) by centrifugation in a clinical centrifuge at 4000 rpm for 10 min. The final PFOA concentration was 2 mol %. Samples containing PFOB were prepared similarly with the following exception. An appropriate volume of PFOB was added to hydrated POPC before freeze−thawing. The final PFOB concentration was 2 mol %. Samples were put in thick-walled 5 or 10 mm NMR tubes with a valve at the top (Wilmad Glass, 1.5 mm wall thickness). The tube interior was then flushed with the appropriate gas for several minutes and then pressurized to 250 psi (17 atm). All pressurized samples were prepared in duplicate; one was pressurized with N_2 and the other with O_2. Relaxation rates due to the presence of O_2 were obtained by subtracting the rates for samples containing N_2 from the rates for samples containing O_2. Control experiments showed that the relaxation rates obtained for samples pressurized with N_2 were the same as those in the presence of atmospheric air.

^{13}C and ^{19}F NMR spectra were recorded at 125.749 and 470.441 MHz, respectively, on a Varian Unity Inova 500 spectrometer. Data were processed with Varian VNMR software, Felix97 (MSI, San Diego, CA) or Nuts (Acorn NMR, Livermore, CA). Spectra were recorded at 25 and 37 °C, and ^{19}F chemical shifts were referenced to external $CFCl_3$. The inversion recovery technique was used to measure spin−lattice relaxation times.[37]

Membrane Localization of PFOB from Paramagnetic Enhancements of Spin−Lattice Relaxation. The bilayer locations of the POPC and PFOA nuclei are known and could be used to localize the nuclei of PFOB by comparison of the spin−lattice relaxation enhancement of PFOB, PFOA, and POPC nuclei due to Gd^{3+} and O_2. Oxygen concentration increases from the surface and the center of bilayers,[23,24] whereas Gd^{3+} is expected to have a maximal concentration near the membrane surface.[22] We measured ^{13}C POPC, ^{19}F

PFOB, and ^{19}F PFOA relaxation rates and used the last two sets of rates to calculate ^{13}C rates. These ^{13}C PFOB and PFOA rates could then be compared with the POPC rates. The Appendix contains theoretical and experimental justification for calculation of ^{13}C PFOB and PFOA spin−lattice relaxation rates based on the analogous ^{19}F rates. The Appendix also contains theoretical justification for interpretation of the spin−lattice rates in terms of the intrabilayer localization of PFOB.

Centrifugation. Extruded bilayer vesicles described above were spun at 50000 rpm (170300*g*) for 2 h in a Sorvall T-1270 rotor and Sorvall OTD65B ultracentrifuge. The bilayers floated to the top of the centrifuge tube and were separated from the clear solution below the bilayers with a Pasteur pipet.

Sample Preparation and ^{2}H and ^{31}P NMR. A mixture of 10% deuterated phosphatidylcholine and 90% POPC was dried overnight under vacuum and then hydrated with 10 mM K_2PO_4, pH 7.0; the phosphatidylcholine concentration was 0.5 M. Samples containing 20 mol % PFOB were prepared by adding an appropriate amount of PFOB to the hydrated phospholipid followed by vortex mixing and seven freeze−thaw cycles. Samples containing smaller amounts of PFOB were prepared as above, but additional phospholipid was added immediately after the PFOB addition step in order to obtain the desired PFOB concentration. The fraction of deuterated lipid was constant.

The NMR spectrometer consisted of an Oxford Instruments 8.45T magnet and primarily Tecmag, Doty Scientific, ENI, and Henry Radio components. MacNMR (Tecmag, Houston) and Nuts (Acorn NMR, Livermore, CA) were used to process the spectra. The quadrupole echo sequence[38] was used to collect ^{2}H NMR spectra at 55.42 MHz. The 90° pulse width was 2.5 μs, the delay between pulses was 40 us, and the sweep width was 200 kHz. The recycle time was 300 ms, and typically 100 000 scans were collected. Free induction decays were apodized with 100 Hz exponential line broadening, zero-filled twice to 16 394 points and Fourier transformed. The phase-cycled Hahn echo pulse sequence[39] was used to collect ^{31}P NMR spectra at 146.15 MHz. The 90° pulse width was 8 μs, the delay between pulses was 50 μs, and the sweep width was 100 kHz. Continuous wave ^{1}H decoupling was used during the free induction decay acquisition time, and the decoupling field strength ($\gamma H_2/(2\pi)$) was 35 kHz. The recycle time was 2 s, and typically 5000 scans were collected. Free induction decays were apodized with 50 Hz exponential line broadening, zero-filled twice to 16 384 points, and Fourier transformed.

Acknowledgment. We thank Ching-Ling Teng and Robert G. Bryant for helpful discussions regarding nuclear magnetic resonance relaxation enhancement. This work was supported by Alliance Pharmaceuticals and NIH Grant GM35215 to D.S.C.

Appendix

The enhancement of the POPC ^{13}C spin−lattice relaxation rates by Gd^{3+} is promoted by both intramolecular and intermolecular interactions. Gd^{3+} binds to the headgroup phosphate of POPC and has strong dipolar interactions with nearby ^{13}C nuclei in the headgroup and glycerol backbone. Dipolar interactions between bound Gd^{3+} and ^{13}C nuclei in the acyl chains are likely to be predominantly intermolecular and therefore modulated by translational diffusion, as is the case for headgroup−acyl chain ^{1}H dipolar interactions in phospholipid membranes.[28,29] As the distance between bound Gd^{3+} and the observed POPC ^{13}C nucleus increases, the dominant relaxation enhancement mechanism will switch from intramolecular to intermolecular. An exact description of the relative contributions of intramolecular and intermolecular interactions to the relaxtion enhancement of all POPC ^{13}C nuclei due to bound Gd^{3+} is not available. However, our interpretation of the relaxation enhancement data in terms of relative distances between bound Gd^{3+} and POPC ^{13}C nuclei does not rely on precise quantitation of intramolecular and intermolecular contributions to relaxation. Other dipolar interactions in the current study that are modulated by translational diffusion include those between bound Gd^{3+} and the ^{19}F nuclei of PFOB and PFOA, those between O_2 and the ^{13}C nuclei of POPC, and those between O_2 and the ^{19}F nuclei of PFOB and PFOA.

Nuclear spin−lattice relaxation due to an electron−nuclear dipolar interaction that has a fixed distance (i.e., intramolecular) is described by[40]

$$T_{1\mathrm{intra}}^{-1} = \frac{2}{15}\gamma_I^2\gamma_S^2\hbar^2\left\{\frac{S(S+1)}{b_r^6}\right\}\{j_2(\omega_S-\omega_I) + 3j_1(\omega_I) + 6j_2(\omega_S+\omega_I)\} \quad (1)$$

where γ_I and γ_S are the nuclear and electron magnetogyric ratios, $\hbar$ is Planck's constant divided by 2π, S is the electron spin quantum number, and b_r is the distance between nuclear (I) and electron (S) spins. The spectral density function for rotational diffusion is

$$j_k(\omega) = \frac{\tau_{ck}}{1+\omega^2\tau_{ck}^2} \quad (2)$$

where ω is the angular resonance frequency and τ_{ck} is

$$1/\tau_{ck} = 1/\tau_R + 1/T_{1S} + 1/T_{2S} \quad (3)$$

where τ_R is the rotational correlation time for the electron−nuclear vector and T_{1S} and T_{2S} are the electron spin−lattice and spin−spin relaxation times, respectively.

Lipid and paramagnetic probe diffusive motions determine the enhancement of the POPC acyl chain ^{13}C and PFOA and PFOB ^{19}F spin−lattice relaxation rates by Gd^{3+} and O_2. The spin−lattice relaxation rate of a nuclear spin in the presence of an independently diffusing electron spin is[41]

$$T_{1\mathrm{inter}}^{-1} = \frac{32\pi}{405}\gamma_I^2\gamma_S^2\hbar^2 S(S+1)\left(\frac{N_a}{1000}\right)\frac{[S]\tau_t p_0}{b^3} \times \{j_2(\omega_S-\omega_I) + 3j_1(\omega_I) + 6j_2(\omega_S+\omega_I)\} \quad (4)$$

where all symbols have the same meaning as above, N_a is Avogadro's number, $[S]$ is the electron spin concentration, p_0 is the probability of collision between the electron and nuclear spins, b is the distance of closest approach of the electron and nuclear spins, and τ_t is the translational correlation time for the electron−nuclear vector and is given by

$$1/\tau_t = 1/\tau_{tI} + 1/\tau_{tS} \quad (5)$$

where τ_{tI} and τ_{tS} are the translational correlation times for the nuclear and electron spins, respectively. Because $T_{1,2S} \leq \tau_t$, the appropriate spectral density function for

nuclear relaxation due to intermolecular interactions with Gd^{3+} and O_2 is

$$j_k(\omega) = \mathrm{Re}\left\{\frac{1+\frac{s}{4}}{1+s+\frac{4s^2}{9}+\frac{s^3}{9}}\right\} \quad (6)$$

with

$$s = b\left[\frac{i\omega + (T_{1S}+T_{2S})^{-1}}{D}\right]^{1/2} \quad (7)$$

where b has the same meaning as above, i is $(-1)^{-1/2}$, ω is the angular resonance frequency, T_{1S} and T_{2S} are the electron spin−lattice and spin−spin relaxation times, and D is the sum of the diffusion coefficients of molecules that contain the I and S spins.

One can use eq 4 to obtain the following relationship between intermolecular spin−lattice relaxation enhancements for ^{19}F and ^{13}C assuming that the spectral density is constant.

$$\frac{T_{1\mathrm{interF}}^{-1}}{T_{1\mathrm{interC}}^{-1}} = \frac{\gamma_F^2 b_C^3}{\gamma_C^2 b_F^3} \quad (8)$$

The subscripts F and C refer to ^{19}F and ^{13}C, respectively. As above, b is the distance of closest approach of the paramagnetic species which enhances relaxation and the relaxing nucleus and is equal to the sum of the van der Waals radii of the interacting species. For the case of O_2, $T_{1\mathrm{interF}}^{-1}/T_{1\mathrm{interC}}^{-1} = 17.5$, and for Gd^{3+}, $T_{1\mathrm{interF}}^{-1}/T_{1\mathrm{interC}}^{-1} = 16.9$. O_2, because of its short electron spin relaxation times and correlation time, dominates the relaxation enhancements observed for PFOB, PFOA, and POPC and consequently conversion of ^{19}F enhancements to ^{13}C enhancements, and comparison of PFOB, PFOA, and POPC enhancements is straightforward. We tested the O_2 case experimentally by measuring the O_2 enhancement of ^{19}F and ^{13}C spin−lattice relaxation in neat PFOB. The ^{19}F relaxation rates were similar for all positions as were the ^{13}C rates. The largest difference between positions was 21%, but the large majority of positions differed by less than 3%. The average experimental $T_{1\mathrm{interF}}^{-1}/T_{1\mathrm{interC}}^{-1}$ was 19.4 ± 0.87. This agrees well with the theoretical value, which is 17.5. Some or all of the difference between the experimental and theoretical values may be due to the possibility that the distance of closest approach between O_2 and ^{13}C is underestimated by the sum of the oxygen and carbon van der Waals radii because the fluorines attached to each carbon may sterically increase the oxygen−carbon distance of closest approach.

Supporting Information Available: ^2H NMR spectra and quadrupolar splittings in the presence and absence of PFOB for both headgroup and chain-labeled POPC. This material is available free of charge via the Internet at http://pubs.acs.org.

References

(1) Long, D. M.; Long, D. C.; Mattrey, R. F.; Long R. A.; Burgan, A. R.; Herrick, W. C.; Shellhamer, D. F. An Overview of Perfluorooctylbromide−Application as a Synthetic Oxygen Carrier and Imaging Agent for X-ray, Ultrasound, and Nuclear Magnetic Resonance. *Biomater., Artif. Cells, Artif. Organs* **1988**, *16*, 411−420.

(2) Nesti, F. D.; Fuhrman, B. P.; Steinhorn, D. M.; Papo, M. C.; Hernan, L. J.; Duffy, L. C.; Fisher, J. E.; Leach, C. L.; Paczan, P. R.; Burak, B. A. Perfluorocarbon-Associated Gas Exchange in Gastric Aspiration. *Crit. Care Med.* **1994**, *22*, 1445−1452.

(3) Tutuncu, A. S.; Faithfull, N. S.; Lachmann, B. Comparison of Ventilatory Support with Intratracheal Perfluorocarbon Administration and Conventional Mechanical Ventilation in Animals with Acute Respiratory Failure. *Am. Rev. Respir. Dis.* **1993**, *148*, 785−792.

(4) Riess, J. Fluorochemical Emulsions. In *Fluorine Chemistry at the Millenium*; Banks, R. E., Ed.; Elsevier: Amsterdam, 2000; pp 385−430.

(5) Obraztsov, V. V.; Grishanova, A. Y.; Shekhtman, D. G.; Sklifas, A. N.; Makarov, K. N. Interaction of Perfluorooctylbromide with Liver Microsomal Monooxygenase. *Biokhimiya* **1993**, *58*, 879−883.

(6) Wolfson, M. R.; Greenspan, J. S.; Shaffer, T. H. Liquid Assisted Ventilation: An Alternative Respiratory Modality. *Pediatr. Pulmonol.* **1998**, *16*, 42−63.

(7) Keipert, P. E. Perfluorochemical Emulsions: Future Alternatives to Transfusion. In *Blood Substitutes: Principles, Methods, Products and Clinical Trials;* Chang, T. M. S., Ed.; Karger Landes Systems: Basel, Switzerland, 1998; pp 127−156.

(8) Spahn, D. R.; van Brempt, R.; Theilmeier, G.; Reibold, J.-P.; Welte, M.; Heinzerling, H.; Birck, K. M.; Keipert, P. E.; Messmer, K. Perflubron Emulsion Delays Blood Transfusions in Orthopedic Surgery. *Anesthesiology* **1999**, *91*, 1195−1208.

(9) Hirschl, R. B.; Tooley, R.; Parent, A. C.; Johnson, K.; Bartlett, R. H. Improvement of Gas Exchange, Pulmonary Function, and Lung Injury with Partial Liquid Ventilation. *Chest* **1995**, *108*, 500−508.

(10) Leach, C. L.; Greenspan, J. S.; Rubenstein, S. D.; Shaffer, T. H.; Wolfson, M. R.; Jackson, J. C.; Delamos, R.; Furman, B. P. Partial Liquid Ventilation with Perflubron in Premature Infants with Severe Respiratory Distress Syndrome. *N. Engl. J. Med.* **1996**, *335*, 761−767.

(11) Colton, D.; Hirschl, R.; Johnson, K.; Till, G.; Bartlett, R. Neutrophil infiltration is reduced during partial perfluorocarbon liquid ventilation in the setting of lung injury. *Surg. Forum* **1994**, *1055*, 668−670.

(12) Croce, M. A.; Fabian, T. C.; Patton, J. H., Jr.; Melton, S. M.; Moore, M.; Trenthem, L. L. Partial Liquid Ventilation Decreases the Inflammatory Response in the Alveolar Environment of Trauma Patients. *J. Trauma* **1998**, *45*, 273−280.

(13) Steinhorn, D. M.; Papo, M. C.; Rotta, A. T.; Aljada, A.; Fuhrman, B. P.; Dandona, P. Liquid Ventilation Attenuates Pulmonary Oxidative Damage. *J. Crit. Care* **1999**, *14*, 20−28.

(14) Smith, D.; Sun, X.; Neslund, G.; Flaim, S. F. Effects of Perflubron (LiquiVent) on Human Leukocyte Activation in Vitro. *Am. J. Respir. Crit. Care Med.* **1997**, *155*, A752.

(15) Thomassen, M. J.; Buhrow, L. T.; Wiedemann, H. P. Perflubron Decreases Cytokine Production by Human Alveolar Macrophages. *Crit. Care Med.* **1997**, *25*, 2045−2047.

(16) Woods, C. M.; Neslund, G.; Kornbrust, E. S.; Flaim, S. F. Perflubron Attenuates Neutrophil Adhesion to Activated Endothelial Cells in Vitro. *Am. J. Physiol.: Lung Cell. Mol. Physiol.* **2000**, *278*, L1008−L1017.

(17) Obraztsov, V. V.; Neslund, G. G.; Kornbrust, E. S.; Flaim, S. F.; Woods, C. M. In Vitro Cellular Effects of Perfluorochemicals Correlate with Their Lipid Solubility. *Am. J. Physiol.: Lung Cell. Mol. Physiol.* **2000**, *278*, 1018−1024.

(18) Koblin, D. D.; Chortkoff, B.; Laster, M. J.; Eger, E. I.; Halsey, M. J.; Ionescu, P. Polyhalogenated and Perfluoroinated Compounds That Disobey the Meyer−Overton Hypothesis. *Anesth. Analg.* **1994**, *79*, 1043−1048.

(19) North, C.; Cafiso, D. Contrasting Membrane Localization and Behavior of Halogenated Cyclobutanes That Follow or Violate the Meyer−Overton Hypothesis of General Anesthetic Potency. *Biophys. J.* **1997**, *72*, 1754−1761.

(20) Tang, P.; Yan, B.; Xu, Y. Different Distribution of Fluorinated Anesthetics and Nonanesthetics in Model Membranes: A ^{19}F NMR Study. *Biophys. J.* **1997**, *72*, 1676−1682.

(21) Shukla, H. P.; Mason, R. P.; Woessner, D. E.; Antich, P. P. A Comparison of Three Commercial Perfluorocarbon Emulsions as High-Field ^{19}F NMR Probes of Oxygen Tension and Temperature. *J. Magn. Reson.* **1995**, *B106*, 131−141.

(22) Bergelson, L. D. Paramagnetic Hydrophilic Probes in NMR Investigations of Membrane Systems. In *Methods in Membrane Biology*; Korn, E. D., Ed.; Plenum Press: New York, 1978; Vol. 9, pp 275−335.

(23) Subczynski, W. K.; Hyde, J. S.; Kusumi, A. Oxygen permeability of phosphatidylcholine−cholesterol membranes. *Proc. Natl. Acad. Sci. U.S.A.* **1989**, *86*, 4474−4478.

(24) Marsh, D. Polarity and permation profiles in lipid membranes. *Proc. Natl. Acad. Sci. U.S.A.* **2001**, *98*, 7777−7782.

(25) Seelig, J.; Macdonald, P. M. Phospholipids and Proteins in Biological Membranes. ^{2}H NMR as a Method To Study Structure, Dynamics, and Interactions. *Acc. Chem. Res.* **1987**, *20*, 221−228.
(26) Bloom, M.; Evans, E.; Mouritsen, O. G. Physical Properties of the Fluid Lipid-Bilayer Component of Cell Membranes: A Perspective. *Q. Rev. Biophys.* **1991**, *24*, 293−397.
(27) Macdonald, P. M. Deuterium NMR and the Topography of Surface Electrostatic Charge. *Acc. Chem. Res.* **1997**, *30*, 196−203.
(28) Huster, D.; Arnold, K.; Gawrisch, K. Investigation of Lipid Organization in Biological Membranes by Two-Dimensional Nuclear Overhauser Enhancement Spectroscopy. *J. Phys. Chem. B*. **1999**, *103*, 243−251.
(29) Huster, D.; Gawrisch, K. NOESY NMR Crosspeaks Between Lipid Headgroups and Hydrocarbon Chains: Spin Diffusion or Molecular Disorder? *J. Am. Chem. Soc.* **1999**, *121*, 1992−1993.
(30) Hubbell, W. L.; Cafiso, D. S.; Altenbach, C. Identifying Conformational Changes with Site-Directed Spin Labeling. *Nat. Struct. Biol.* **2000**, *7*, 735−739.
(31) Prosser, R. S.; Luchette, P. A.; Westerman, P. W. Using O_2 To Probe Membrane Immersion Depth by ^{19}F NMR. *Proc. Natl. Acad. Sci. U.S.A.* **2000**, *97*, 9967−9971.
(32) Prosser, R. S.; Luchette, P. A.; Westerman, P. W.; Rozek, A.; Hancock, R. E. W. Determination of Membrane Immersion Depth with O_2: A High-Pressure ^{19}F NMR Study. *Biophys. J.* **2001**, *80*, 1406−1416.
(33) White, S. H.; Wimley, W. C. Hydrophobic Interactions of Peptides with Membrane Interfaces. *Biochim. Biophys. Acta* **1998**, *1376*, 339−352.
(34) Kaiser, R. D.; London, E. Location of Diphenylhexatriene (DPH) and Its Derivatives within Membranes: Comparison of Different Fluorescence Quenching Analyses of Membrane Depth. *Biochemistry* **1998**, *37*, 8180−8190.
(35) Luchette, P. A.; Prosser, R. S.; Sanders, C. R. Oxygen as a Paramagnetic Probe of Membrane Protein Structure by Cysteine Mutagenesis and ^{19}F NMR Spectroscopy. *J. Am. Chem. Soc.* **2002**, *124*, 1778−1781.
(36) Cui, S. T.; Siepmann, H. D.; Cochran, H. D.; Cummings, P. T. Intermolecular Potentials and Vapor−Liquid Phase Equilibria of Perfluorinated Alkanes. *Fluid Phase Equilib.* **1998**, *146*, 51−61.
(37) Freeman, R.; Hill, H. D. W.; Kaptein, R. An Adaptive Scheme for Measuring NMR Spin−Lattice Relaxation Times. *J. Magn. Reson.* **1972**, *7*, 82−98.
(38) Davis, J. H. The Description of Membrane Lipid Conformation, Order and Dynamics by ^{2}H NMR. *Biochim. Biophys. Acta* **1983**, *737*, 117−171.
(39) Rance, M.; Byrd, R. A. Obtaining High Fidelity Spin-1/2 Powder Spectra in Anisotropic Media: Phase-Cycled Hahn Echo Spectroscopy. *J. Magn. Reson.* **1983**, *52*, 221−240.
(40) Solomon, I. Relaxation Processes in a System of Two Spins. *Phys. Rev.* **1955**, *99*, 559−565.
(41) Freed, J. Dynamic Effects of Pair Correlation Functions on Spin Relaxation by Translational Diffusion in Liquids. II. Finite Jumps and Independent T_1 Processes. *J. Chem. Phys.* **1978**, *68*, 4034−4037.

JM020278X